IEEE Access
Multidisciplinary ⋮ Rapid Review ⋮ Open Access Journal

Received May 31, 2020, accepted June 12, 2020, date of publication June 22, 2020, date of current version July 2, 2020.

Digital Object Identifier 10.1109/ACCESS.2020.3003915

Impact Angle Constraint Dual-Layer Adaptive Guidance Law With Actuator Faults

QIANCAI MA[1], YI JI[1,2], ZHIQI NIU[3], QIUXIONG GOU[3], AND LIANGYU ZHAO[1]

[1]School of Aerospace Engineering, Beijing Institute of Technology, Beijing 100081, China
[2]Beijing Key Laboratory of UAV Autonomous Control, Ministry of Education, Beijing Institute of Technology, Beijing 100081, China
[3]Xi'an Modern Control Technology Research Institute, Xi'an 710065, China

Corresponding author: Liangyu Zhao (zhaoly@bit.edu.cn)

This work was supported in part by the National Natural Science Foundation of China under Grant 11532002 and Grant 11202023, and in part by the Hong Jian Foundation of the Xi'an Modern Control Technology Research Institute.

ABSTRACT To intercept maneuvering target considering impact angle constraint and actuator faults, a novel three-dimensional (3D) guidance law is proposed in this paper. To guarantee the interception, the multi-variable super-twisting-algorithm-like (STA-like) is adopted in the proposed guidance law, so as to drive the line-of-sight (LOS) angle to the desired value and its rate to zero in finite time in both pitch and azimuth directions. However, it is usually a difficult task for STA-like to select the proper design parameters, and the necessary disturbance gradient for STA-like is also not clearly known, owing to realistic actuator faults and the independence between missile and target. Moreover, the actuator faults in this paper are formulated as disturbances in the control scheme, and the necessary disturbance gradient for STA-like is not clearly known as well. To solve these problems, a multi-variable dual-layer adaptive scheme is employed to adjust the control gains and guarantees its precision. The theoretical analysis and numerical simulation results demonstrate the effectiveness of the proposed guidance law. The combination of STA-like and adaptive theory in the presented guidance law for the first time can guarantee the successful interception and can generate precise and robust control signal simultaneously with impact angle constraint and actuator faults consideration.

INDEX TERMS Guidance law, actuator fault, impact angle, adaptive dual-layer control, finite-time convergence.

I. INTRODUCTION

In recent decades, maneuverable target accurate interception problem is still an important part of guidance law design. According to [1]–[3], successful accurate interception usually requires impact angle constraint, especially for maneuvering targets like tactical ballistic missiles.

Due to the easy implementation and efficiency, the proportional navigation guidance law (PNG) and its variants in [4]–[6] have been widely used to design guidance law. However, owing to the independent target maneuvers, the performance of PNG is unsatisfactory. In the opened technical literature [7], [8], PNG is a fairly effective method during the interception for stationary or slow-maneuvering target. But considering the perturbations resistance and target maneuvering, PNG may not be the optimal solution for impact angle constraint.

The associate editor coordinating the review of this manuscript and approving it for publication was Choon Ki Ahn.

With the development of modern nonlinear control theory, optimal algorithm [9], [10], H_∞ theory [11] and other methods [12]–[17] were introduced to solve the interception problem. Because of the high robustness against external disturbances and uncertainties of systematic parameters, sliding mode control (SMC) is a powerful tool for robust guidance law design with the characteristic of the finite time convergence. In [18], guidance laws were developed using the traditional SMC. Considering delayed LOS rate measurement, Kim *et al.* [19] and Yamasaki *et al.* [20] proposed sliding mode guidance laws to deal with impact angle constraint. Shin and Song [21] presented a linear sliding surface to synthesize a guidance law to impose desired intercept angle for head-on and tail-chase scenarios. To realize finite time convergence, terminal sliding mode (TSM) were employed in the guidance law design in [22], [23]. Then, aiming at the singularity and slow-convergence problem of the TMS guidance law, nonsingular TSM (NTSM) algorithms were adopted to design guidance laws to solve these problems,

and ensure desired impact angle, in [24]–[26]. However, according to the work in [23], [27], it should be known that the proper control parameters of the TMS guidance law and NTMS guidance law are both difficulty to choose. In [28], [29], adaptive control laws for obtaining specified impact angle were proposed, and applied into reentry guidance of a hypersonic vehicle. The optimal SMC guidance laws to satisfy the terminal impact angle constraint were proposed in [30], where the equivalent control part was formulated by model predictive control. However, owing to its inherent chattering, SMC-based guidance laws may cause undesired high-frequency chattering within missile acceleration commands. To avoid this situation, super-twisting algorithm (STA) was employed to design guidance law [31]. As a second order continuous SMC algorithm, STA generates the continuous control function that drives the sliding variable and its derivative to zero in finite time in the presence of the smooth matched disturbances with bounded gradient. The only need is that the boundary of the gradient should be known in advance. However, owing to the strong independence between the missile and the target, the boundary of the disturbance gradient is hard to measure during the interception, especially for targets with high speed maneuver. Thus, the precision of the guidance law based on STA is hard to guarantee. To acquire proper disturbance boundary, Edwards and Shtessel [32] and Utkin and Poznyak [33] proposed adaptive-gain STA (ASTA) control laws. The ASTA can handle the perturbed plant dynamics with additive disturbance and unknown boundary in finite convergence time. Then, Edwards and Shtessel [34] and Shtessel *et al.* [35] proposed a dual-layer adaptive STA-like control algorithm, which can estimate disturbance boundary precisely enough and can minimize the degree of over-estimation of the bounds.

Real manipulation disturbances is also an important factor affecting the performance of guidance law. In [36], [37], the guidance law with autopilot lag consideration were proposed. In [38], [39], the guidance laws with seeker's field-of-view constraint were researched. According to the work in [40], [41], as a kind of common manipulation disturbance, actuator faults may cause severe performance deterioration, or even system instability. In [42], [43], different methods were introduced to deal with actuator faults. Then in [44], [45], fault-tolerant control theories were introduced into guidance laws design. However, combined target maneuvers with actuator faults, the boundary of the disturbance may be much more easily over-estimated.

Inspired by above work, a novel impact angle constraint dual-layer adaptive guidance law with actuator faults is proposed in this paper. The main contribution of this paper can be concluded as follows: (1) Different from the traditional PNG, the proposed guidance law can achieve the interception with desired impact angles in finite time; (2) A dual-layer adaptive scheme is employed to get more precisely estimated disturbance information due to the actuator faults and target maneuvers; (3) A multi-variable dual-layer adaptive control scheme is developed to realize impact angles constraint in both pitch and azimuth directions.

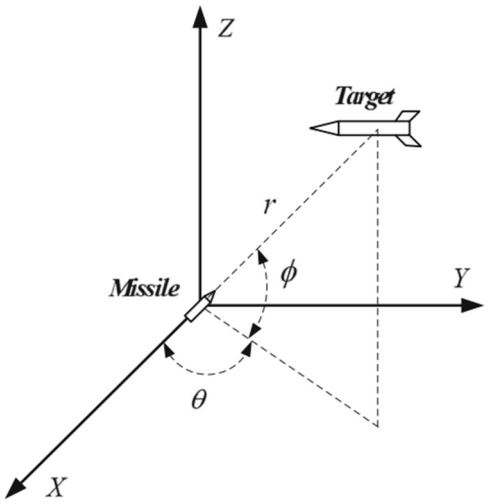

FIGURE 1. Three-dimensional homing guidance geometry.

The rest of this paper is organized as follows. In Section II, the preliminary including the mathematic model of the three-dimensional homing guidance engagement phase, model of the actuator faults and some notations are introduced. In Section III, a multi-variable dual adaptive STA-like guidance scheme and the design method of dual-layer adaption gain are declared. Simulation results are presented and analyzed in Section VI. Some conclusions are made in the last section.

II. PROBLEM STATEMENT

In this section, kinematics model of missile-target guidance system and actuator faults during the engagement phase are presented for the later guidance design law design. Moreover, some notations are also considered for further application to facilitate the design.

A. ENGAGEMENT KINEMATICS

According to the work in [46], the three-dimensional (3D) homing guidance geometry is shown as Fig. 1, where r denotes the LOS distance between the missile and the target, θ and ϕ represent the pitch and azimuth of the LOS angles, respectively. Then, the engagement dynamic systems can be expressed as follow,

$$\ddot{r} = r\dot{\phi}^2 + r\dot{\theta}^2\cos^2\phi \tag{1}$$

$$\ddot{\theta} = -\frac{2\dot{r}\dot{\theta}}{r} + 2\dot{\phi}\dot{\theta}\tan\phi + \frac{a_{T\theta}}{r\cos\phi} - \frac{a_{M\theta}}{r\cos\phi} \tag{2}$$

$$\ddot{\phi} = -\frac{2\dot{r}\dot{\phi}}{r} - \dot{\theta}^2\sin\phi\cos\phi + \frac{a_{T\phi}}{r} - \frac{a_{M\phi}}{r} \tag{3}$$

where, $a_{M\theta}$ and $a_{M\phi}$ represent the commanded acceleration components of the missile in the three-dimensional coordinates, respectively. $a_{T\theta}$ and $a_{T\phi}$ denote the target accelerations. In this study, assuming that the signals r, $\dot{r}$, θ and ϕ can

be measured by the strapdown system, the main objective of the guidance law is to successfully intercept the target with impact angle constraint.

In the notational form, the equation (2) and equation (3) can be rewritten as,

$$\begin{bmatrix} \ddot{\theta} \\ \ddot{\phi} \end{bmatrix} = \boldsymbol{F} + \boldsymbol{B}\boldsymbol{a}_{\boldsymbol{M}} + \boldsymbol{\Delta} \tag{4}$$

where

$$\boldsymbol{F} = \begin{bmatrix} -\frac{2\dot{r}\dot{\theta}}{r} + 2\dot{\phi}\dot{\theta}\tan\phi \\ -\frac{2\dot{r}\dot{\phi}}{r} - \dot{\theta}^2\sin\phi\cos\phi \end{bmatrix}, \quad \boldsymbol{B} = \begin{bmatrix} -\frac{1}{r\cos\phi} & 0 \\ 0 & -\frac{1}{r} \end{bmatrix}$$

$$\boldsymbol{a}_{\boldsymbol{M}} = \left[a_{M\theta}, a_{M\phi}\right]^T, \quad \boldsymbol{\Delta} = \left[\Delta_\theta, \Delta_\phi\right]^T = \left[\frac{a_{T\theta}}{r\cos\phi}, \frac{a_{T\phi}}{r}\right]^T$$

$$\boldsymbol{a}_{\boldsymbol{T}} = \left[a_{T\theta}, a_{T\phi}\right]^T, \tag{5}$$

in which $\boldsymbol{a}_{\boldsymbol{M}}, \boldsymbol{a}_{\boldsymbol{T}}$ and $\boldsymbol{\Delta}$ represent the control input, target maneuvers and system uncertainties, respectively.

Due to physical limitations, during a realistic pursuit-evasion engagement, under the initial condition of $\dot{r} < 0$ with a suitable guidance gain, the LOS angular rate is also bounded except for the point when the interception is realized ($r = 0$ is the impact point). Furthermore, the interception occurs when $r \neq 0$ due to the target being a particular size. Thus this singular point does not occur in real world application. The impact is assumed to be happened when the distance vector between the missile and the target r belongs to the interval $[r_{\min}, r_{\max}] = [0.5, 1.0]$ m.

Remark 1: From system (4), it can be concluded that $\phi = \pm\pi/2$ are two singular point of the guidance system. It follows [45] that during engagement phase the scenario $\phi = \pm\pi/2$ are not the stable equilibrium cases, and the guidance trajectory crosses these points and will not stay there.

B. KINEMATICA OF ACTUATOR FAILURE

Based on control theory and control system, actuator faults are usually divided into two types: additive faults and out of control [44]. The former referred that the bounded fault enter control channels in an additive way, while the other one referred actuator loses its effectiveness.

Taking actuator faults into account, the total acceleration $\boldsymbol{a}_{\boldsymbol{M}}$ can be formulated as a new form:

$$\boldsymbol{a}_{\boldsymbol{M}} = \boldsymbol{a}_{\boldsymbol{M}}^{\boldsymbol{n}} + \boldsymbol{G}\left(t - T_f^0\right)\boldsymbol{a}_{\boldsymbol{M}}^{\boldsymbol{f}} \tag{6}$$

where, $\boldsymbol{a}_{\boldsymbol{M}}^{\boldsymbol{n}}$ denotes the nominal acceleration, $\boldsymbol{G}\left(t - T_f^0\right)\boldsymbol{a}_M^f$ represents the deviation in acceleration due to the presence of actuator faults. $\boldsymbol{G}\left(t - T_f^0\right)$ represents the time profiles of a fault that occurs at some unknown time. $\boldsymbol{a}_{\boldsymbol{M}}^{\boldsymbol{f}}$ is the nonlinear fault function. $\boldsymbol{G}\left(t - T_f^0\right)$ is a diagonal matrix,

$$\boldsymbol{G}\left(t - T_f^0\right) = diag\left[g_\theta\left(t - T_{f1}^0\right), g_\phi\left(t - T_{f2}^0\right)\right] \tag{7}$$

where, $g_i\ (i = \theta, \phi)$ is a function denoting a fault time profile and is governed by the equation as follows,

$$g_i\left(t - T_{fi}^0\right) = \begin{cases} 0 & if\ t < T_{fi}^0 \\ 1 - e^{-a_i\left(t - T_{fi}^0\right)} & if\ t \geq T_{fi}^0 \end{cases} \tag{8}$$

where the scalar $a_i > 0$ is the unknown fault evolution rate. For large a_i, the time profile of g_i which approaches a step function, could denote an abrupt fault in the model. And small a_i represents slow development faults, also known as initial faults.

To cope with the system as equation (4) in the presence of the actuator faults as equation (6), a new disturbance vector is defined as

$$\boldsymbol{d} = \boldsymbol{B}\boldsymbol{G}\left(t - T_f^0\right)\boldsymbol{a}_{\boldsymbol{M}}^{\boldsymbol{f}} + \boldsymbol{\Delta} \tag{9}$$

and $\boldsymbol{d} = \left[d_\theta \ \ d_\phi\right]^T$.

Hence, system (4) can be rewritten as follow,

$$\begin{bmatrix} \ddot{\theta} \\ \ddot{\phi} \end{bmatrix} = \boldsymbol{F} + \boldsymbol{B}\boldsymbol{a}_{\boldsymbol{M}} + \boldsymbol{d} \tag{10}$$

This completes the guidance system in the presence of actuator faults during the engagement phase.

Let θ_d and ϕ_d denote the desired LOS angles and are constants, $\boldsymbol{x}_1$ and $\boldsymbol{x}_2$ represent the LOS angle error and the LOS angle rate error, which are defined by

$$\begin{aligned} \boldsymbol{x}_1 &= \left[x_{1\theta} \ \ x_{1\phi}\right]^T = \left[\theta - \theta_d \ \ \phi - \phi_d\right]^T \\ \boldsymbol{x}_2 &= \dot{\boldsymbol{x}}_1 = \left[x_{2\theta} \ \ x_{2\phi}\right]^T = \left[\dot{\theta} \ \ \dot{\phi}\right]^T \end{aligned} \tag{11}$$

Take equation (11) into the system (10),

$$\begin{aligned} \dot{x}_{1\theta} &= x_{2\theta} \\ \dot{x}_{1\phi} &= x_{2\phi} \\ \dot{x}_{2\theta} &= -\frac{2\dot{r}x_{2\theta}}{r} + 2x_{2\phi}x_{2\theta}\tan\phi + \frac{a_{T\theta}}{r\cos\phi} - \frac{a_{M\theta}^n}{r\cos\phi} - \frac{a_{M\theta}^f}{r\cos\phi} \\ \dot{x}_{2\phi} &= -\frac{2\dot{r}x_{2\phi}}{r} - x_{2\theta}^2\sin\phi\cos\phi + \frac{a_{T\phi}}{r} - \frac{a_{M\phi}^n}{r} - \frac{a_{M\phi}^f}{r} \end{aligned} \tag{12}$$

and the system (12) can be rewritten as a following second-order system,

$$\begin{aligned} \dot{\boldsymbol{x}}_1 &= \boldsymbol{x}_2 \\ \dot{\boldsymbol{x}}_2 &= \boldsymbol{F} + \boldsymbol{B}\boldsymbol{a}_{\boldsymbol{M}} + \boldsymbol{d} \end{aligned} \tag{13}$$

The objective of this study can be described as designing acceleration commands $\boldsymbol{a}_M$ for system (10) aiming to drive the LOS angle error $\boldsymbol{x}_1$ and LOS angle rate $\boldsymbol{x}_2$ error converge to zero in finite time.

Remark 2: Owing to the physical limits, the acceleration of the target is bounded. Hence, the dumped disturbance $\boldsymbol{d}$ and its first-order time derivative in system (10) is continuous and bounded but unknown, i.e., there are two positive vectors

$$\boldsymbol{d}_{max} = \left[d_{max,\theta} \ \ d_{max,\phi}\right]^T, \quad \dot{\boldsymbol{d}}_{max} = \left[\dot{d}_{max,\theta} \ \ \dot{d}_{max,\phi}\right]^T \tag{14}$$

which satisfy

$$|d_i| \leq d_{\max,i}, \left|\dot{d}_i\right| \leq \dot{d}_{\max,i}, (i = \theta, \phi) \tag{15}$$

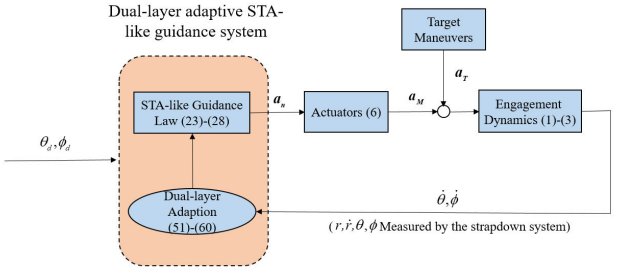

FIGURE 2. Flowchart of the proposed guidance law.

III. DUAL-LAYER ADAPTIVE STA-LIKE GUIDANCE LAW DESIGN

In this section, a new framework of a multi-variable adaptive STA-like guidance law with linear term and dual-layer adaptive methodology is introduced. The flowchart of proposed guidance scheme considering both impact angle constraint and actuator faults is shown in Fig. 2.

A. DESIGN OF A MULTI-VARIABLE ADAPTIVE STALIKE GUIDANCE LAW

In [43], finite time convergence is defined as follow,

Lemma 1 (See [46]): Considering the nonlinear system $\dot{x} = f(x,t)$, $x \in R^n$. Assume the existence of a continuous and positive definite function $V(x)$,

$$\dot{V}(x) + \lambda_1 V(x) + \lambda_2 V^{\theta}(x) \le 0 \tag{16}$$

where $\lambda_1, \lambda_2 > 0$ and $0 < \theta < 1$ are constants. $x(t_0) = x_0$, in which t_0 is the initial time. Then, the time of the system states arriving at the equilibrium point T satisfies the following inequality:

$$T \le \frac{1}{\lambda_1 (1-\theta)} \ln\left(1 + \frac{\lambda_1}{\lambda_2} V^{1-\theta}(x_0)\right) \tag{17}$$

Inspired by the work in [47], define the terminal sliding manifold as,

$$\boldsymbol{s} = \dot{\boldsymbol{x}} + \boldsymbol{b}_1 \boldsymbol{x} + \boldsymbol{b}_2 |\boldsymbol{x}|^{\boldsymbol{b}_3} \mathbf{sign}(\boldsymbol{x}) \tag{18}$$

where

$$\begin{aligned} \dot{\boldsymbol{x}} &= \left[\dot{x}_1 \;\; \dot{x}_2\right]^T \\ |\boldsymbol{x}| &= \left[|\dot{x}_1| \;\; |\dot{x}_2|\right]^T \end{aligned} \tag{19}$$

and

$$\begin{aligned} \boldsymbol{b}_1 &= \begin{bmatrix} b_{11} & 0 \\ 0 & b_{12} \end{bmatrix} \in \mathbb{R}^{2\times 2}, \quad \boldsymbol{b}_2 = \begin{bmatrix} b_{21} & 0 \\ 0 & b_{22} \end{bmatrix} \in \mathbb{R}^{2\times 2}, \\ \boldsymbol{b}_3 &= \begin{bmatrix} b_{31} & 0 \\ 0 & b_{32} \end{bmatrix} \in \mathbb{R}^{2\times 2} \end{aligned} \tag{20}$$

Moreover, $\mathbf{sign}(\boldsymbol{x})$ is the sign function, and the definition is shown in APPENDIX.

The time derivative of $\boldsymbol{s}$ can be expressed as,

$$\begin{aligned} \dot{\boldsymbol{s}} &= \ddot{\boldsymbol{x}} + \boldsymbol{b}_1 \dot{\boldsymbol{x}} + \boldsymbol{b}_2 \boldsymbol{b}_3 |\boldsymbol{x}|^{\boldsymbol{b}_3 - I} \dot{\boldsymbol{x}} \\ &= \bar{\boldsymbol{F}}(\boldsymbol{x}) + \boldsymbol{B} \boldsymbol{a}_M^n + \boldsymbol{d} \end{aligned} \tag{21}$$

and

$$\bar{\boldsymbol{F}}(\boldsymbol{x}) = \begin{bmatrix} -\dfrac{2\dot{r}\dot{\theta}}{r} + 2\dot{\theta}\dot{\phi}\tan\phi + b_{11}\dot{\theta} + b_{21}b_{31}|\theta|^{b_{31}-1}\dot{\theta} \\ -\dfrac{2\dot{r}\dot{\phi}}{r} + \dot{\theta}^2 \sin\phi\cos\phi + b_{12}\dot{\phi} + b_{22}b_{32}|\phi|^{b_{32}-1}\dot{\phi} \end{bmatrix} \tag{22}$$

Inspired by the single-variable ASTA control theory in [35], a multi-variable dual-layer adaptive STA-like guidance law is formulated, according to the system (21),

$$\begin{aligned} \boldsymbol{a}_M^n &= -\boldsymbol{B}^{-1}\left(\bar{\boldsymbol{F}}(\boldsymbol{x}) + \boldsymbol{u}\right) \\ \boldsymbol{u}(t) &= -\boldsymbol{\alpha}(t) \circ \frac{\boldsymbol{s}}{\|\boldsymbol{s}\|^{1/2}} + \boldsymbol{y} + \Phi(\boldsymbol{s}, \boldsymbol{L}) \\ \dot{\boldsymbol{y}}(t) &= -\boldsymbol{\beta}(t) \circ \frac{\boldsymbol{s}}{\|\boldsymbol{s}\|} \end{aligned} \tag{23}$$

where "$\circ$" is schur product symbol, and the definition is shown in APPENDIX, and

$$\boldsymbol{\alpha}(t) = \left[\alpha_1(t) \;\; \alpha_2(t)\right]^T, \quad \boldsymbol{\beta}(t) = \left[\beta_1(t) \;\; \beta_2(t)\right]^T \tag{24}$$

and the gain $\boldsymbol{\alpha}(t)$ and $\boldsymbol{\beta}(t)$ are defined as,

$$\begin{aligned} \boldsymbol{\alpha}(t) &= \boldsymbol{\alpha}_0 \sqrt{\boldsymbol{L}(t)} \\ \boldsymbol{\beta}(t) &= \boldsymbol{\beta}_0 \boldsymbol{L}(t) \end{aligned} \tag{25}$$

where $\boldsymbol{L}(t)$ is adaptive element vector, which

$$\boldsymbol{L}(t) = \left[l_1(t) \;\; l_2(t)\right]^T \tag{26}$$

$\boldsymbol{\alpha}_0$ and $\boldsymbol{\beta}_0$ are positive constants, which

$$\boldsymbol{\alpha}_0 = \left[\alpha_{01} \;\; \alpha_{02}\right]^T, \quad \boldsymbol{\beta}_0 = \left[\beta_{01} \;\; \beta_{02}\right]^T \tag{27}$$

and $\Phi(\boldsymbol{s}, \boldsymbol{L})$ is defined as

$$\Phi(\boldsymbol{s}, \boldsymbol{L}) = -\frac{\dot{\boldsymbol{L}}(t)}{\boldsymbol{L}(t)} \circ \boldsymbol{s} \tag{28}$$

Take equation (10), equation (18) and equation (23) into consideration, assume that adaptive element vector $\boldsymbol{L}(t)$ is bounded with a non-overestimated but unknown value a_0 and the elements are selected so as to satisfy the initial adaptive element vector $\boldsymbol{L}_0(t) > \dot{\boldsymbol{d}}$, which is defined as

$$\boldsymbol{L}_0(t) = \left[l_{01}(t) \;\; l_{02}(t)\right] \tag{29}$$

Define following matrices as

$$\begin{aligned} \boldsymbol{A}_0 &= \begin{bmatrix} -\frac{1}{2}\alpha_0 & \frac{1}{2} \\ -\beta_0 & 0 \end{bmatrix}, \quad \boldsymbol{B}_0 = \begin{bmatrix} 0 \\ 1 \end{bmatrix}, \\ \boldsymbol{C}_0 &= \begin{bmatrix} 1 & 0 \end{bmatrix}, \quad \boldsymbol{P} = \begin{bmatrix} p_1 & p_2 \\ p_2 & p_3 \end{bmatrix} \end{aligned} \tag{30}$$

where, $\boldsymbol{P}$ is a symmetric positive matrix, and satisfies $p_1 > 0$, $p_2 > 0$ and $p_1 p_2 > p_2^2$.

Motivated by [34], a novel multi-variable dual-layer adaptive STA-like guidance law is proposed, and can drive the LOS angle and its rates converge to desired value in both pitch and azimuth directions.

Theorem 1: The proposed multi-variable dual-layer adaptive STA-like guidance law in equation (23) can drive the missile intercept maneuvering targets with the desired impact angle in a finite time $\boldsymbol{T_{reach}}$ in both pitch and azimuth directions, if the gains α_0 and β_0 are selected to satisfy the following inequality,

$$\boldsymbol{P}\boldsymbol{A}_0 + \boldsymbol{A}_0^T\boldsymbol{P} + \boldsymbol{P}\boldsymbol{B}_0\boldsymbol{B}_0^T\boldsymbol{P} + \boldsymbol{C}_0^T\boldsymbol{C}_0 < \mu\boldsymbol{P} \tag{31}$$

and $\boldsymbol{T}_{reach}$ is formulated as

$$\boldsymbol{T_{reach}} \leq \frac{2}{\gamma}\boldsymbol{V}^{1/2}(0) \tag{32}$$

where

$$\boldsymbol{\gamma} = \mu L_0\sqrt{\lambda_{\min}(\boldsymbol{P})}, \quad \boldsymbol{\gamma} = \begin{bmatrix}\boldsymbol{\gamma}_1 & \boldsymbol{\gamma}_2\end{bmatrix} \tag{33}$$

and μ is a positive constant.

Proof: To prove the proposed guidance law in equation (23) can drive the LOS angle and its rates converge to desired value in both pitch and azimuth directions, employ the notation

$$z = \begin{bmatrix} z_1 \\ z_2 \end{bmatrix} = \begin{bmatrix} \sqrt{\boldsymbol{L}} \circ \boldsymbol{s} / \|\boldsymbol{s}\|^{\frac{1}{2}} \\ \boldsymbol{y} \end{bmatrix} \tag{34}$$

Then, equation (18) can be formulated as following equation through the auxiliary vector.

$$\dot{\boldsymbol{s}} = -\alpha_0 z_1 + z_2 + \Phi(\boldsymbol{s}, \boldsymbol{L}) + \boldsymbol{d} \tag{35}$$

Take the derivative of the equation (34) with the respect to time yields

$$\begin{cases} \dot{z}_1 = \dfrac{-\boldsymbol{\alpha}(t)}{2\|\boldsymbol{s}\|^{1/2}} \circ z_1 + \dfrac{\sqrt{\boldsymbol{L}}}{2\|\boldsymbol{s}\|^{1/2}} \circ z_2 \\ \dot{z}_2 = -\dfrac{\sqrt{\boldsymbol{L}}}{\|\boldsymbol{s}\|^{1/2}} \circ \left(-\dfrac{\boldsymbol{\beta}(t)}{\boldsymbol{L}} \circ z_1 + \tilde{\boldsymbol{\xi}}(t) \right) \end{cases} \tag{36}$$

since

$$\frac{\dot{\boldsymbol{L}}(t)}{2\sqrt{\boldsymbol{L}(t)}} \circ \frac{\boldsymbol{s}}{\|\boldsymbol{s}\|^{1/2}} + \frac{\sqrt{\boldsymbol{L}(t)}}{2\|\boldsymbol{s}\|^{1/2}} \circ \Phi(\boldsymbol{s}, \boldsymbol{L}) = 0 \tag{37}$$

In equation (36), $\boldsymbol{\xi}(t)$ is the re-defined uncertainty, which is the deviation of the actuator faults disturbance.

$$\tilde{\boldsymbol{\xi}}(t) = \frac{\|\boldsymbol{s}\|^{1/2}}{\sqrt{\boldsymbol{L}}} \circ \boldsymbol{\xi}(t) \tag{38}$$

since $|z_1| = \sqrt{\boldsymbol{L}}\|\boldsymbol{s}\|^{1/2}$, $\tilde{\boldsymbol{\xi}}(t)$ satisfies

$$\left|\tilde{\boldsymbol{\xi}}(t)\right| = \frac{\|\boldsymbol{s}\|^{1/2}}{\sqrt{\boldsymbol{L}}} \circ \left|\tilde{\boldsymbol{\xi}}(t)\right| \leq \frac{\|\boldsymbol{\xi}(t)\|}{\sqrt{\boldsymbol{L}}} \circ |z_1| \tag{39}$$

Then, system equation (36) can be transformed to

$$\dot{z} = \boldsymbol{D}(s) \circ \left(\boldsymbol{A}_0 z + \boldsymbol{B}_0\tilde{\boldsymbol{\xi}}\right) \tag{40}$$

where

$$\boldsymbol{A}_0 = \begin{bmatrix} -\dfrac{1}{2}\alpha_0 & \dfrac{1}{2} \\ -\beta_0 & 0 \end{bmatrix}, \quad \boldsymbol{B}_0 = \begin{bmatrix} 0 \\ 1 \end{bmatrix},$$
$$\boldsymbol{D}(s) = \sqrt{\boldsymbol{L}}/\|s\|^{1/2} \tag{41}$$

Take a Lyapunov function candidate:

$$\boldsymbol{V} = \frac{1}{2}\boldsymbol{z}^{\boldsymbol{T}}\boldsymbol{P}\boldsymbol{z} \tag{42}$$

along the solution of equation (36) when $s \neq 0$, yielding

$$\begin{aligned} \dot{\boldsymbol{V}} &= \boldsymbol{D}(s)\left(z^T\left(\boldsymbol{A}_0^T\boldsymbol{P} + \boldsymbol{P}\boldsymbol{A}_0\right)z + 2z^T\boldsymbol{P}\boldsymbol{B}_0\tilde{\boldsymbol{\xi}}(t)\right) \\ &\leq \boldsymbol{D}(s)\left(z^T\left(\boldsymbol{A}_0^T\boldsymbol{P} + \boldsymbol{P}\boldsymbol{A}_0 + \boldsymbol{P}\boldsymbol{B}_0\boldsymbol{B}_0^T\boldsymbol{P} + \boldsymbol{C}_0^T\boldsymbol{C}_0\right)z + \tilde{\boldsymbol{\xi}}^2(t)\right) \end{aligned} \tag{43}$$

According to the inequality (39), it can be seen

$$\left|\tilde{\boldsymbol{\xi}}(t)\right| \leq \frac{\|\boldsymbol{\xi}(t)\|}{\boldsymbol{L}(t)}|\boldsymbol{x}_1| \leq |\boldsymbol{x}_1| \tag{44}$$

Hence,

$$\begin{aligned} \dot{\boldsymbol{V}} &= \boldsymbol{D}(s)\left(z^T\left(\boldsymbol{A}_0^T\boldsymbol{P} + \boldsymbol{P}\boldsymbol{A}_0 + \boldsymbol{P}\boldsymbol{B}_0\boldsymbol{B}_0^T\boldsymbol{P}\right)z + z_1^2\right) \\ &= \boldsymbol{D}(s)z^T\left(\boldsymbol{A}_0^T\boldsymbol{P} + \boldsymbol{P}\boldsymbol{A}_0 + \boldsymbol{P}\boldsymbol{B}_0\boldsymbol{B}_0^T\boldsymbol{P} + \boldsymbol{C}_0^T\boldsymbol{C}_0\right)z \end{aligned} \tag{45}$$

Once α_0 and β_0 satisfy the inequality,

$$\boldsymbol{P}\boldsymbol{A}_0 + \boldsymbol{A}_0^T\boldsymbol{P} + \boldsymbol{P}\boldsymbol{B}_0\boldsymbol{B}_0^T\boldsymbol{P} + \boldsymbol{C}_0^T\boldsymbol{C}_0 < \mu\boldsymbol{P} \tag{46}$$

there is

$$\dot{\boldsymbol{V}} \leq -\frac{\mu\sqrt{\boldsymbol{L}}}{\|\boldsymbol{s}\|^{1/2}} \circ \boldsymbol{V}$$

According to the definition of $\boldsymbol{V}$,

$$\begin{aligned} &\lambda_{\min}(\boldsymbol{P})\|\boldsymbol{z}\|_2^2 \leq \boldsymbol{V} \leq \lambda_{\max}(\boldsymbol{P})\|\boldsymbol{z}\|_2^2 \\ &\sqrt{\boldsymbol{L}}\|\boldsymbol{s}\|^{1/2} < \|\boldsymbol{z}_1\| < \|\boldsymbol{z}\| \end{aligned} \tag{47}$$

Therefore,

$$\|\boldsymbol{s}\|^{1/2} \leq \sqrt{\frac{\boldsymbol{V}}{\lambda_{\min}(\boldsymbol{P})\boldsymbol{L}}} \tag{48}$$

and,

$$\dot{\boldsymbol{V}} \leq -\mu\lambda_{\min}^{1/2}(\boldsymbol{P})\boldsymbol{L} \circ \boldsymbol{V}^{1/2} \leq -\gamma\boldsymbol{V}^{1/2} \tag{49}$$

In the inequality (37), $\gamma > 0$. According to **Lemma 1**, the proposed guidance law is stabilized in finite-time.

Remark 3: The multi-variable adaptive STA-like guidance law (23)∼(28) can achieve the finite time missile interception with desired impact angles in both pitch and azimuth directions, and the dual-layer adaptive gain should be chosen and bounded.

B. DUAL-LAYER ADAPTION GAIN L(t) DESIGN

According to the above section, the proposed guidance scheme can drive the system state $\boldsymbol{x}$ and $\dot{\boldsymbol{x}}$ converge to zero using a properly chosen bounded adaptive function $\boldsymbol{L}(t)$. In this section, the adaptive function $\boldsymbol{L}(t)$ will be designed.

In [34], a so-called dual-layer adaptive algorithm is proposed to design the adaptive function $\boldsymbol{L}(t)$. The dual layer approaches rely on equivalent control technique. However, the proposed guidance law requires multi-variable form.

Hence, a multi-variable discontinuous term during the sliding in equation (23) is developed as follow,

$$\boldsymbol{\beta}(t) \circ \left.\frac{\boldsymbol{s}}{\|\boldsymbol{s}\|}\right|_{eq} = \boldsymbol{\xi}(t) \tag{50}$$

which is referred to as the equivalent control in the proposed guidance law.

As a theoretic conception, the equivalent control cannot be accurately measured or calculated in real time. Based on low pass filtering technology, it can be approximately estimated using the following first-order differentiator with switched signal,s

$$\dot{\bar{\boldsymbol{u}}}_{eq}(t) = \frac{1}{\tau} \circ \left(\boldsymbol{\beta}(t) \circ \frac{\boldsymbol{s}}{|\boldsymbol{s}|} - \bar{\boldsymbol{u}}_{eq}(t)\right) \tag{51}$$

where $\boldsymbol{\tau} = \begin{bmatrix} \tau_1 & \tau_2 \end{bmatrix}^T$ is an arbitrary given positive constant which represents the frequency of the low pass filter, $\bar{\boldsymbol{u}}_{eq}(t)$ represents the estimated value of the equivalent control. As a result, the bounded total disturbance $\dot{\boldsymbol{d}}$ can be precisely estimated in both pitch and azimuth directions.

Inspired by the work in [34], define a new vector variable as,

$$\boldsymbol{\delta}(t) = \boldsymbol{L}(t) - \frac{1}{a\beta_0} \circ \left|\bar{\boldsymbol{u}}_{eq}(t)\right| - \boldsymbol{\varepsilon} \tag{52}$$

where the scalar $a = \begin{bmatrix} a_1 & a_2 \end{bmatrix}^T$ is chosen to satisfy

$$0 < a < 1/\beta_0 < 1 \tag{53}$$

and $\boldsymbol{\varepsilon} = \begin{bmatrix} \varepsilon_1 & \varepsilon_2 \end{bmatrix}^T$ is small and positive, which is chosen to ensure

$$\frac{1}{a\beta_0} \circ \left|\bar{\boldsymbol{u}}_{eq}(t)\right| + \boldsymbol{\varepsilon}/2 > \left|\boldsymbol{u}_{eq}(t)\right| \tag{54}$$

Then, the adaptive control element $\boldsymbol{L}(t)$ can be presented as

$$\boldsymbol{L}(t) = \boldsymbol{l}_0 + \boldsymbol{l}(t) \tag{55}$$

where

$$\begin{aligned} \boldsymbol{l}_0 &= \begin{bmatrix} l_{01} & l_{02} \end{bmatrix}^T \\ \boldsymbol{l}(t) &= \begin{bmatrix} l_1(t) & l_2(t) \end{bmatrix}^T \end{aligned} \tag{56}$$

$\boldsymbol{l}(t)$ is the time varying term and satisfies,

$$\dot{\boldsymbol{l}}(t) = -\boldsymbol{\rho}(t) \circ \mathbf{sign}(\boldsymbol{\delta}(t)) \tag{57}$$

The time varying scalar in equation (57) is defined by

$$\boldsymbol{\rho}(t) = \boldsymbol{q}_0 + \boldsymbol{q}(t) \tag{58}$$

where

$$\begin{aligned} \boldsymbol{q}_0 &= \begin{bmatrix} q_{01} & q_{02} \end{bmatrix}^T \\ \boldsymbol{q}(t) &= \begin{bmatrix} q_1(t) & q_2(t) \end{bmatrix}^T \end{aligned} \tag{59}$$

and the time varying component $\boldsymbol{q}(t)$ satisfies

$$\dot{\boldsymbol{q}}(t) = \boldsymbol{\gamma} \circ |\boldsymbol{\delta}(t)| \tag{60}$$

where

$$\boldsymbol{\gamma} = \begin{bmatrix} \gamma_1 & \gamma_2 \end{bmatrix}^T, \quad \gamma_1 > 0, \gamma_2 > 0 \tag{61}$$

The main conclusion of this section is summarized as following theorem.

Theorem 2: Subject the system equation (7) into lump uncertainty vector $\boldsymbol{d}(t)$ and its time derivative $\boldsymbol{\xi}(t)$, which satisfies

$$\|\boldsymbol{\xi}(t)\| \le a_0, \quad \left\|\dot{\boldsymbol{\xi}}(t)\right\| \le a_1$$

the dual-layer adaptive algorithm in equation (51)∼(60) ensures that the adaptive element vector $\boldsymbol{L}(t) \ge |\boldsymbol{\xi}(t)|$ in finite time.

Proof: For the convenience of demonstration, an auxiliary variable is defined as

$$\boldsymbol{e}(t) = \frac{a_1}{a\beta_0}\boldsymbol{I}_2 - \boldsymbol{q}(t) \tag{62}$$

Take the derivative of $\delta(t)$ with the respect to time yields

$$\begin{aligned} \dot{\boldsymbol{\delta}}(t) &= \dot{\boldsymbol{l}}(t) - \frac{1}{a\beta_0} \circ \frac{d}{dt}\left|\bar{\boldsymbol{u}}_{\boldsymbol{eq}}(t)\right| \boldsymbol{I}_2 \\ &= \dot{\boldsymbol{l}}(t) - \frac{1}{a\beta_0} \circ \frac{d}{dt}|\boldsymbol{\xi}(t)| \boldsymbol{I}_2 \end{aligned} \tag{63}$$

Further, it follows from the equations (52), (62) and (63) that

$$\begin{aligned} &\boldsymbol{\delta}(t) \circ \dot{\boldsymbol{\delta}}(t) \\ &\le \boldsymbol{\delta}(t) \circ \dot{\boldsymbol{l}}(t) + \frac{1}{a\beta_0} \circ \frac{d}{dt}|\boldsymbol{\delta}(t)| \\ &= -\boldsymbol{q}_0 \circ |\boldsymbol{\delta}(t)| - \boldsymbol{q} \circ |\boldsymbol{\delta}(t)| + \frac{1}{a\beta_0} \circ \frac{d}{dt}|\boldsymbol{\delta}(t)| \\ &= -\boldsymbol{q}_0 \circ |\boldsymbol{\delta}(t)| + \boldsymbol{e}(t) \circ |\boldsymbol{\delta}(t)| \end{aligned} \tag{64}$$

To discuss the ultimate uniform global boundedness of the dynamical system, following Lyapunov function is taken into account.

$$\boldsymbol{V}(\boldsymbol{\delta}, \boldsymbol{e}) = \frac{1}{2}\boldsymbol{\delta} \circ \boldsymbol{\delta} + \frac{1}{2\gamma}\boldsymbol{e} \circ \boldsymbol{e} \tag{65}$$

Take its derivative along the trajectories of $\delta(t)$ and $e(t)$ it follows that,

$$\begin{aligned} &\dot{\boldsymbol{V}}(\boldsymbol{\delta}, \boldsymbol{e}) \\ &= \boldsymbol{\delta} \circ \dot{\boldsymbol{\delta}} + \frac{1}{\gamma}\boldsymbol{e} \circ \dot{\boldsymbol{e}} \\ &\le -\boldsymbol{q}_0 \circ |\boldsymbol{\delta}(t)| - \boldsymbol{e}(t) \circ |\boldsymbol{\delta}(t)| + \frac{1}{\gamma}\boldsymbol{e}(t) \circ (-\gamma \circ |\boldsymbol{\delta}(t)|) \\ &= -\boldsymbol{q}_0 \circ |\boldsymbol{\delta}(t)| \end{aligned} \tag{66}$$

Since $\dot{\boldsymbol{V}}(\boldsymbol{\delta}, \boldsymbol{e}) \le 0$, one can imply that $\boldsymbol{\delta}(t)$ and $\boldsymbol{e}(t)$ have their own bound, and $\boldsymbol{\delta}(t) \to \mathbf{0}_2$ as $t \to \infty$. As a result there exists a finite time t_0 such that $|\boldsymbol{\delta}(t)| \le \boldsymbol{\varepsilon/2}$ holds for $t > t_0$. It follows from the definition of $\boldsymbol{\delta}(t)$ in equation (63) that

$$|\boldsymbol{\delta}(t)| = \left|\boldsymbol{L}(t) - \frac{1}{a\beta_0} \circ \left|\bar{\boldsymbol{u}}_{eq}(t)\right| - \boldsymbol{\varepsilon}\right| < \frac{\boldsymbol{\varepsilon}}{2} \tag{67}$$

Thus

$$\boldsymbol{L}(t) - \frac{1}{a\beta_0} \circ \left|\bar{\boldsymbol{u}}_{eq}(t)\right| - \boldsymbol{\varepsilon} > -\frac{\boldsymbol{\varepsilon}}{2} \tag{68}$$

It follows from $a\beta_0 < 1$, that

$$\boldsymbol{L}(t) > \frac{1}{a\beta_0} \circ \left|\bar{\boldsymbol{u}}_{eq}(t)\right| + \frac{\boldsymbol{\varepsilon}}{2} > \left|\bar{\boldsymbol{u}}_{eq}(t)\right| + \frac{\boldsymbol{\varepsilon}}{2} > |\boldsymbol{\xi}(t)| \tag{69}$$

Furthermore, according to the definition of $\delta(t)$ in equation (52) it follows:

$$\begin{aligned} |\boldsymbol{L}(t)| &< \frac{1}{a\beta_0} \circ \left|\bar{\boldsymbol{u}}_{eq}(t)\right| + \frac{1}{2}\boldsymbol{\varepsilon} \\ &< |\boldsymbol{\delta}(t)| + \frac{1}{a\beta_0} \circ \left|\bar{\boldsymbol{u}}_{eq}(t)\right| + \frac{1}{2}\boldsymbol{\varepsilon} \\ &< |\boldsymbol{\delta}(t)| + \frac{a_1}{a\beta_0}\boldsymbol{I}_2 + \frac{1}{2}\boldsymbol{\varepsilon} \end{aligned} \tag{70}$$

This completes the proof.

Remark 4: From the control algorithm equation (23)∼(28) and the dual-layer adaptive scheme equation (51)∼(60), the proposed guidance law can achieve the finite time missile interception with desired impact angles, and the developed multi-variable dual-layer adaptive control scheme can provide more precisely estimated disturbance information due to the actuator faults and target maneuvers. Moreover, the multi-variable dual-layer adaptive control scheme is creatively presented in the proposed guidance law to guarantee impact angles constraint in both pitch and azimuth directions.

IV. SIMULATION RESULTS

In this section, the effectiveness of the proposed guidance law considering impact angle constraint and actuator faults are demonstrated through numerical simulations by examples of homing engagement phase in an impact angel constraint accurate guidance mission. The simulations are performed in the MATLAB® platform by using a fourth-order Runge-Kutta solver with fixed step size 0.001s.

A. SIMULATIONS FOR ACTUATOR FAULTS

To verify the effectiveness of the proposed guidance law, simulations for the different degree control information loss of actuator faults are performed.

Let the actuator in θ direction loses 0%, 5%, 10%, 15% and 25% of control information when the terminal guidance phase begins, i.e. $u_{f\theta} = 0$, $u_{f\theta} = -0.05u_{n\theta}$, $u_{f\theta} = -0.1u_{n\theta}$, $u_{f\theta} = -0.15u_{n\theta}$, $u_{f\theta} = -0.25u_{n\theta}$, while the actuator in ϕ direction loses 10% of control information i.e. $u_{f\phi} = -0.1u_{n\phi}$.

Let the actuator in ϕ direction loses 0%, 5%, 10%, 15% and 25% of control information when the terminal guidance phase begins, i.e. $u_{f\phi} = 0$, $u_{f\phi} = -0.05u_{n\phi}$, $u_{f\phi} = -0.1u_{n\phi}$, $u_{f\phi} = -0.15u_{n\phi}$, $u_{f\phi} = -0.25u_{n\phi}$, while the actuator in θ direction loses 10% of control information i.e. $u_{f\theta} = -0.1u_{n\theta}$.

Simulations are set as follows: (1) initial relative range: $r(0) = 9000$m; (2) initial relative velocity: $\dot{r}(0) = -600$m/s; (3) initial LOS angles: $\theta(0) = \pi/6, \phi(0) = \pi/12$; (4) initial LOS angular rates: $\dot{\theta}(0) = 1/15$rad/s, $\dot{\phi}(0) = 1/20$rad/s; (5) desired LOS angle $\theta_d = 45°, \phi_d = 25°$.

The target maneuver satisfies.

$$a_{T\theta} = -30\text{m/s}^2, a_{T\phi} = -30\text{m/s}^2.$$

TABLE 1. Design parameters.

Parameter	Value	Parameter	Value
α_{01}, α_{02}	5	q_{01}, q_{02}	0.1
β_{01}, β_{02}	1.2	ε_{01} ε_{02}	0.05
τ_1, τ_2	0.1	b_{11} b_{12}	4
a_1, a_2	0.75	b_{21} b_{22}	3
γ_1, γ_2	0.08	b_{31} b_{32}	2.3
l_{01}, l_{02}	0.055	μ_1 μ_2	0.8

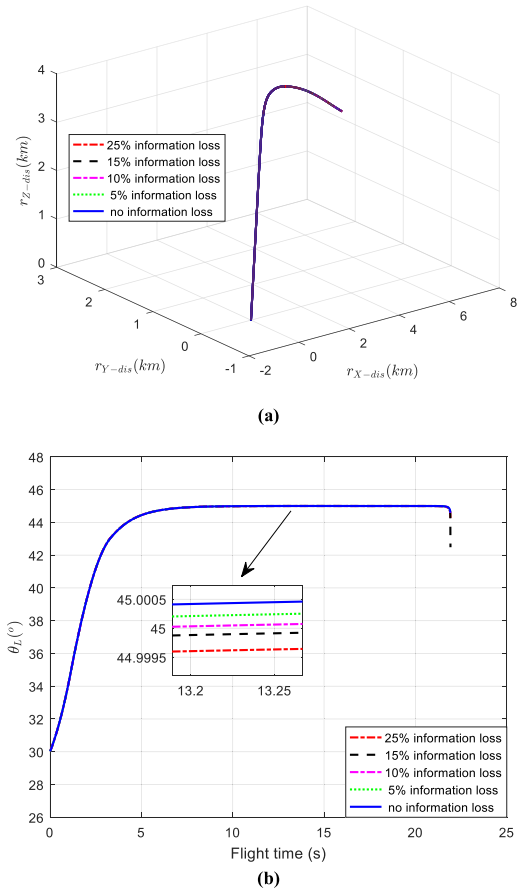

FIGURE 3. Simulation results of different degree of control information loss in θ direction: (a) Relative distance trajectories; (b) LOS angle.

The parameters of the proposed guidance law are given as Table 1.

Fig. 3 shows the trajectories of the relative distance between missile and target and the LOS angle θ_L for different degrees of control information loss in θ direction. Fig. 3(a) shows that the distances in X, Y and Z directions all converge to zero, which indicate that the missile can intercept the target successfully for different degrees of control information loss in θ direction. Fig. 3(b) shows that when actuator in ϕ direction loses 10% of information of control and the actuator in θ direction loses 0%, 5%, 10%, 15% and 25% of information

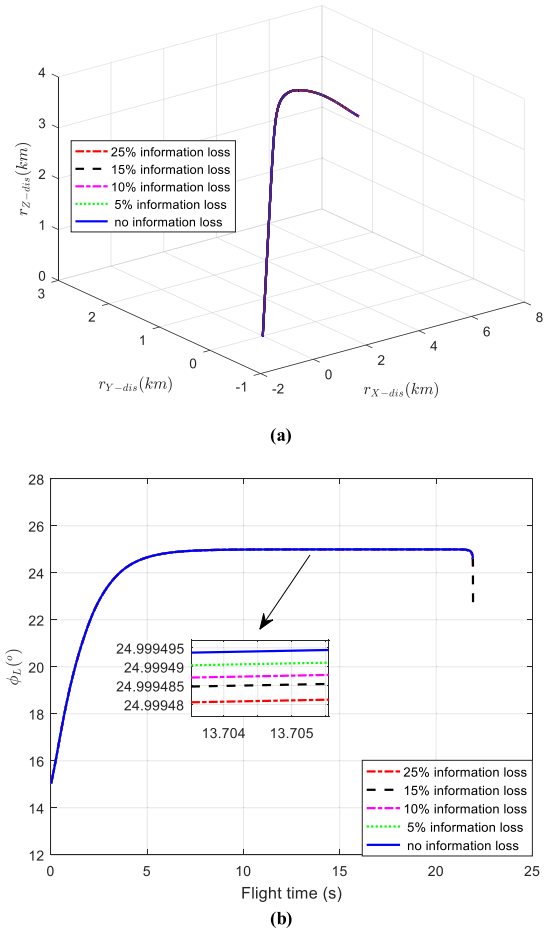

FIGURE 4. Simulation results of different degree of control information loss in ϕ direction: (a) Relative distance trajectories; (b) LOS angle.

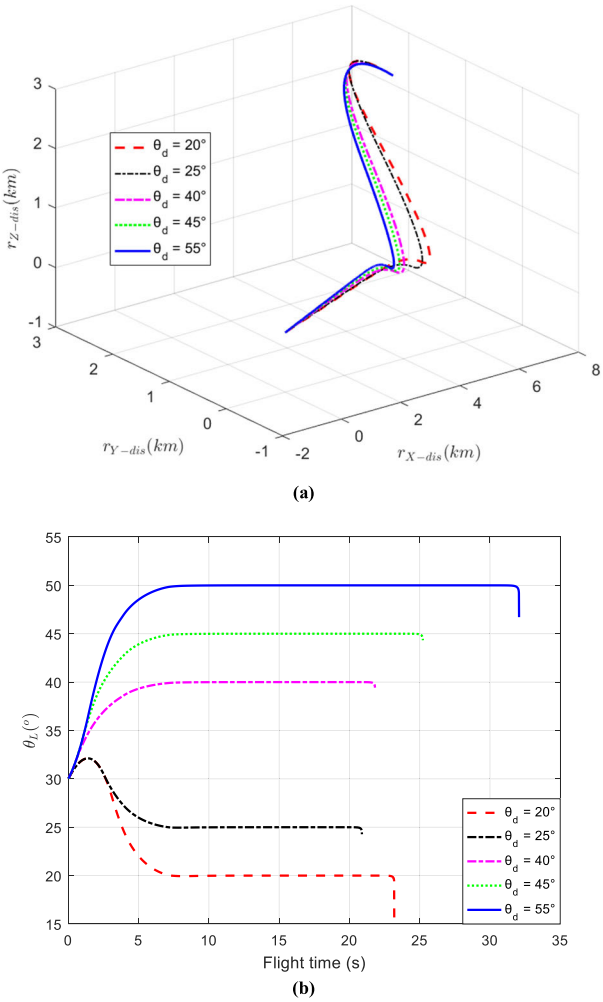

FIGURE 5. Simulation results of different desired impact angles in θ direction: (a) Relative distance trajectories; (b) LOS angle.

of control, all of the θ_L can converge to the desired angles precisely in no more than 14s. The convergence time of θ_L is affected by the different degree of control information loss.

Fig. 4 shows the trajectories of the relative distance between missile and target and the LOS angle ϕ_L for different degrees of control information loss in ϕ direction. Fig. 4(a) shows that the distances in X, Y and Z directions all converge to zero, which indicate that that the missile can intercept the target successfully for different degrees of control information loss in ϕ direction. Fig. 4(b) shows that when actuator in θ direction loses 10% of control information and the actuator in ϕ direction loses 0%, 5%, 10%, 15% and 25% of control information, all of the ϕ_L can converge to the desired angles precisely in no more than 14s. The convergence time of θ_L is affected by the different degrees of control information loss.

B. SIMULATIONS FOR IMPACT ANGLE CONSTRAINTS AND ACTUATOR FAULTS

To test the terminal impact angle constraint properties of the guidance law, simulations considering actuator faults for different desired impact angles with the same initial LOS angles are performed. Let the desired impact angles θ_d be 20°, 25°, 40°, 45° and 55°, when the $\phi_d = 5°$. Let the desired impact angles ϕ_d be -10°, -5°, 5°, 10°, and 15°, when the $\theta_d = 35°$.

Simulations are set as follows: (1)initial relative range: $r\,(0) = 9000$m; (2)initial relative velocity: $\dot{r}\,(0) = -600$m; (3)initial LOS angles: $\theta\,(0) = \pi/6, \phi\,(0) = \pi/12$; (4)initial LOS angular rates: $\dot{\theta}\,(0) = 1/15$rad/s, $\dot{\phi}\,(0) = 1/20$rad/s. The target maneuver satisfies $a_{T\theta} = -30\text{m/s}^2$, $a_{T\phi} = -30\text{m/s}^2$; the actuator faults: the actuator in θ direction loses 25% of information of control when the terminal guidance phase begins, i.e. $u_{f\theta} = -0.25u_{n\theta}$ while the actuator in ϕ direction loses 25% of information of control, i.e. $u_{f\phi} = -0.25u_{n\phi}$. The parameters of the proposed guidance law with the impact angle constraint are same as in Sect. VI. A.

Fig. 5 shows the trajectories of the relative distance between missile and target and the LOS angle θ_L. Fig. 5(a) shows that the distances in X, Y and Z directions all converge to zero, which indicate that the missile can intercept the target successfully for different desired impact angles. Fig. 5(b) shows that when $\phi_d = 5°$ and θ_d be 20°, 25°, 40°, 45° and 55°, all of the θ_L can converge to different desired angles

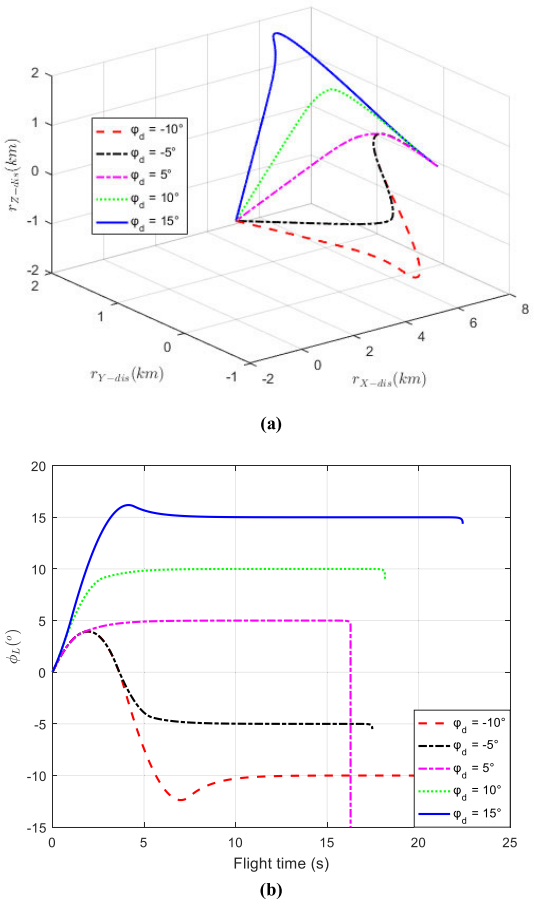

FIGURE 6. Simulation results of different desired impact angles in ϕ direction: (a) Relative distance trajectories; (b) LOS angle.

precisely in no more than 35s. The convergence time of θ_L is affected by the different desired impact angles.

Fig. 6 shows the trajectories of the relative distance between missile and target and the LOS angle ϕ_L. Fig. 6(a) shows that the distances in X, Y and Z directions all converge to zero, which indicate that the missile can intercept the target successfully for different desired impact angles. Fig. 6(b) shows that when $\theta_d = 35°$ and ϕ_d be $-10°$, $-5°$, $5°$, $10°$ and $15°$, all of the ϕ_L can converge to different desired angles precisely in no more than 25s. The convergence time of θ_L is affected by the different desired impact angles.

C. COMPARION WITH OTHER GUIDANCE LAWS

To further verify the effectiveness of the proposed guidance law, a FTC guidance law in [46] and a novel transformed PNG law [50] are used as comparison, which can provide reasonable acceleration control command. In order to indicate results of the guidance law, two engagement cases are studied here, and the performance of impact angle constraint are tested as well.

The FTC is defined in the equation below,

$$\boldsymbol{a_M} = \boldsymbol{B}^{-1}\left\{-\boldsymbol{f}\left(\boldsymbol{x}\right) + \boldsymbol{u}\right\},$$

TABLE 2. Flight time and miss distance.

Guidance Law	Case1		Case2	
	Fight time	Miss distance	Fight time	Miss distance
The proposed	19.792s	0.6743m	19.949s	0.5613m
FTC	18.092s	0.9352m	18.386s	0.9096m
PNGL	16.679s	0.6792m	16.884s	0.7237m

$$\boldsymbol{u}\left(t\right) = -k_1\left(t\right)\frac{\boldsymbol{x}\left(t\right)}{\left\|\boldsymbol{x}\left(t\right)\right\|^2} - k_2\left(t\right)\boldsymbol{x} + \boldsymbol{\varsigma},$$
$$\dot{\boldsymbol{\varsigma}} = -k_3\left(t\right)\frac{\boldsymbol{x}}{\left\|\boldsymbol{x}\left(t\right)\right\|^{1/2}} - k_4\left(t\right)\boldsymbol{x} \tag{71}$$

where the adaptive gains $k_i\left(t\right)$ $(i = 1, 2, 3, 4)$ are designed as,

$$k_1\left(t\right) = c_1\sqrt{L\left(t\right)}, k_2\left(t\right) = c_2 L\left(t\right),$$
$$k_3\left(t\right) = c_3 L\left(t\right), k_4\left(t\right) = c_4 L^2\left(t\right) \tag{72}$$

with an adaptive law

$$\dot{L}\left(t\right) = m\mathbf{sign}\left(\left\|\boldsymbol{x}\right\| - \boldsymbol{\varepsilon}\right) \tag{73}$$

where $m > 0$ is used to regulate the adaptive process, $L \geq 0$ is defined as adaptive parameter, ε is a small value to ensure that $\boldsymbol{L}$ will be bounded. And the positive constants $c_i (i = 1, 2, 3, 4)$ are satisfied with following condition,

$$9c_1^2c_2^2 + 8c_2^2c_3 < 4c_3c_4 \tag{74}$$

where the parameters in FTC guidance law are selected as $c_1 = 1$, $c_2 = 0.5$, $c_3 = 2$, $c_4 = 1$, $\varepsilon = 0.2$ and $m = 0.8t$, respectively.

The transformed PNG law is defined as,

$$\boldsymbol{a_M} = \begin{bmatrix} -N_1\dot{r}\dot{\theta} + f_1\mathrm{sign}\left(\dot{\theta}\right) + M\left|\dot{\theta}\right|^k\mathrm{sign}\left(\dot{\theta}\right) \\ -N_2\dot{r}\dot{\phi} + f_2\mathrm{sign}\left(\dot{\phi}\right) + M\left|\dot{\phi}\right|^k\mathrm{sign}\left(\dot{\phi}\right) \end{bmatrix} \tag{75}$$

where the parameters in PNG are selected as $N_1 = 3$, $N_2 = 3, f_1 = 50, f_2 = 50, M = 10$ and $k = 0.5$, respectively.

Two kinds of target maneuver were taken into account to demonstrate the general applicability and robustness of the proposed guidance laws, which could be expressed as follows,

Case 1: the target maneuver is constant,

$$a_{T\theta} = -30\mathrm{m/s}^2, \quad a_{T\phi} = -30\mathrm{m/s}^2;$$

Case 2: the target maneuver follows the sinusoidal components,

$$a_{T\theta} = -20\sin\left(2\pi t\right)\mathrm{m/s}^2, \quad a_{T\phi} = -20\sin\left(2\pi t\right)\mathrm{m/s}^2$$

The initial conditions for different cases are selected as follow: (1)initial relative range: $r\left(0\right) = 9000$m; (2)initial relative velocity: $\dot{r}\left(0\right) = -600$m; (3)initial LOS angles: $\theta\left(0\right) = \pi/6$, $\phi\left(0\right) = \pi/12$;(4)initial LOS angular rates: $\dot{\theta}\left(0\right) = 1/15$rad/s, $\dot{\phi}\left(0\right) = 1/20$rad/s;(5) desired LOS angles: $\theta_d = 40°$, $\phi_d = 10°$.

The parameters of the proposed guidance law with the impact angle constraint are same as in Sect. VI. A.

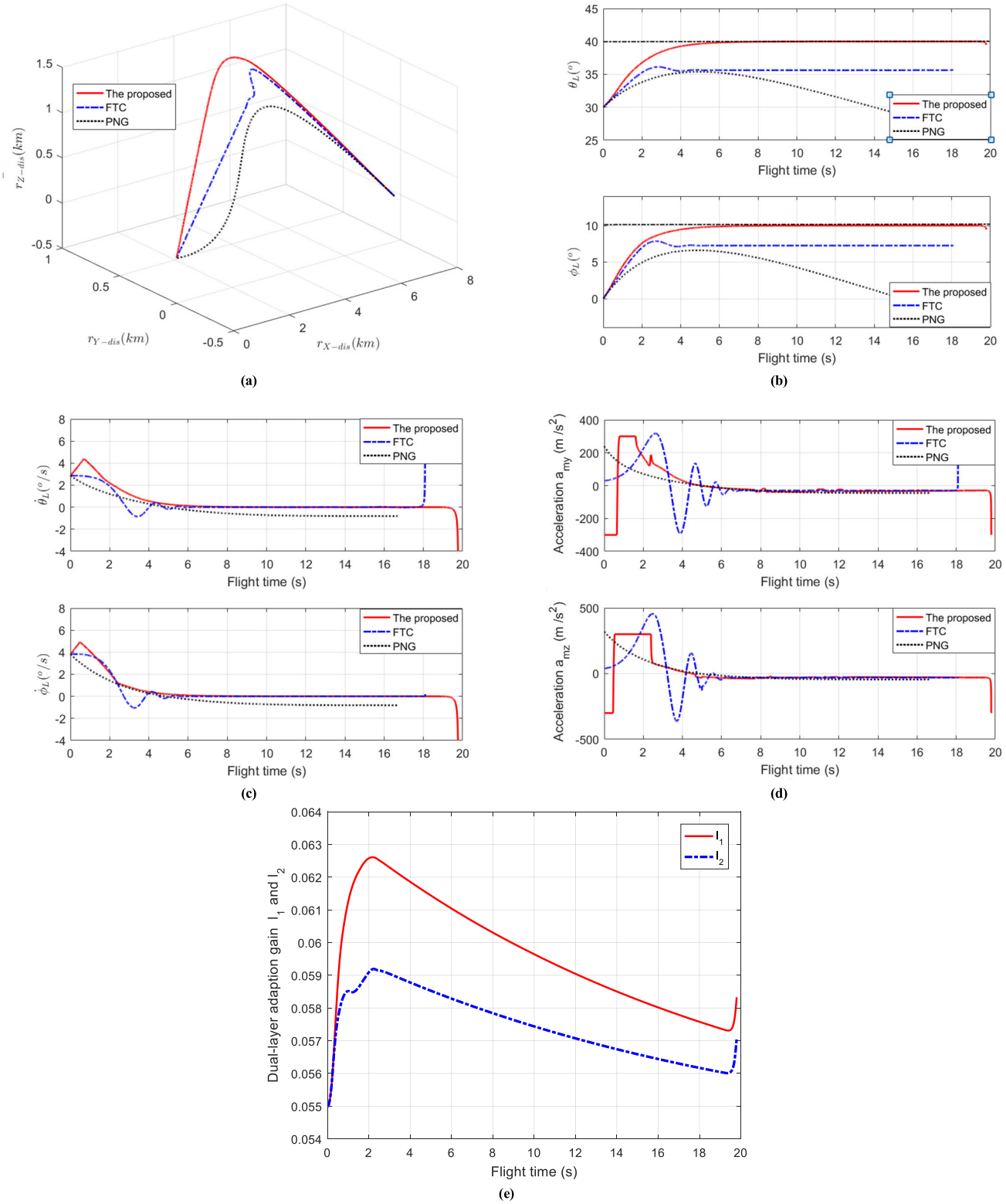

FIGURE 7. Simulation results of Case 1. (a) Relative distance trajectories (b) LOS angle curves (c) LOS angular rate curves (d) Missile acceleration profiles (e) Profiles of dual-layer adaptive gain *L*.

For **case 1**, the simulation results are shown in Fig. 7, and the information of miss distance and flight time is given in Table 2. Fig. 7(a) shows that the relative distance trajectories under three different guidance laws and the distances in X, Y and Z directions all converge to zero, which indicate that all of the three missiles can get rid of the influence of actuator

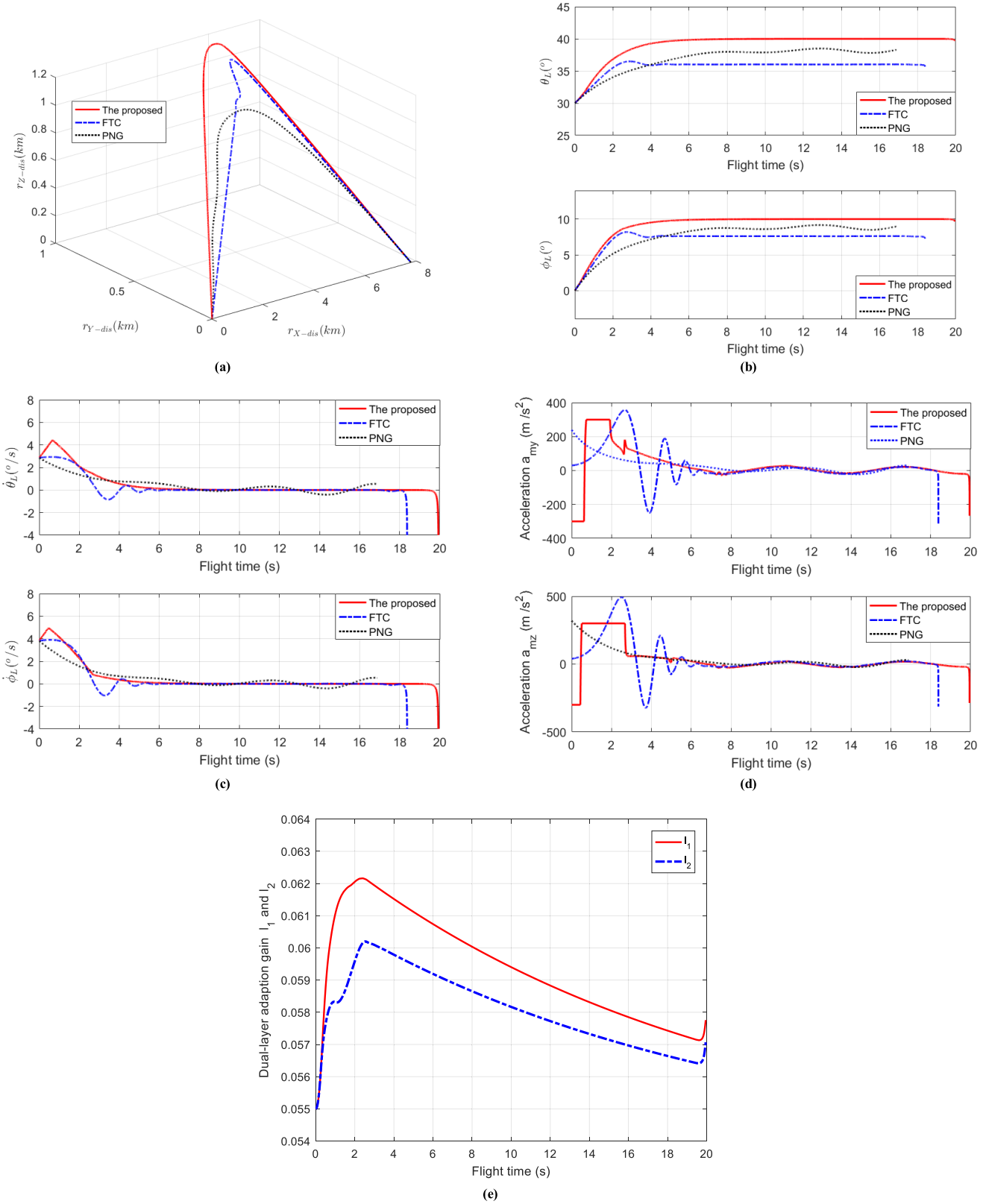

FIGURE 8. Simulation results of Case 2. (a) Relative distance trajectories (b) LOS angle curves (c) LOS angular rate curves (d) Missile acceleration profiles (e) Profiles of dual-layer adaptive gain *L*.

faults for **case 1** and intercept the target successfully, even though the flight paths are different. Fig. 7(b) shows the curves of θ_L and ϕ_L, using three different guidance laws. It is shown that the FTC and PNG cannot guarantee the convergence of the LOS angles, but the proposed guidance law can drive the LOS angles converge to desired values in two directions. Fig. 7(c) shows the LOS angle rate under three guidance laws all converge to zero. Fig. 7(d) shows the acceleration of the missile during the engagement, and the curves of $a_{M\theta}$ and $a_{M\phi}$ show the accelerations of the missile are all in reasonable scales. Fig. 7(e) shows that magnitude of the dual-layer adaptive gain $\boldsymbol{L}$ is bounded and gradually converging. The information of miss distance and flight time is given in Table.2. Summarizing all the above pictures in Fig. 7, it is concluded that actuator faults can influence the performance of the guidance laws which does not consider the practical constraints, and the proposed guidance law can get rid of the influence of actuator faults. Besides, the proposed guidance law can also lead the missile intercept the target with reasonable accelerations. At the same time, the presented guidance law can also guarantee that the LOS angles and angular rates converge to desired values with preferable convergence performances in finite time.

For **case 2**, the simulation results are shown in Fig. 8, and the information of miss distance and flight time is given in Table.2. Fig. 8(a) shows that the relative distance trajectories under three different guidance laws and the distances in X, Y and Z directions all converge to zero, which indicate that all of the three missiles can get rid of the influence of actuator faults for **case 2** and intercept the target successfully, even though the flight paths are different. Fig. 8(b) shows that the curves of LOS angle θ_L and ϕ_L converge to desired values under the proposed guidance law. Fig. 8(c) shows that the LOS angle rate under three guidance laws all converge to zero. Fig. 8(d) shows the acceleration of the missile during the engagement; Fig. 8(e) shows that magnitude of the dual-layer adaptive gain $\boldsymbol{L}$ is bounded and gradually converging. The information of miss distance and flight time is given in Table 2. Similar to **case 1**, the results of **case 2** also show that the proposed guidance law can intercept the target with impact angle constraint and actuator faults. The curves of $a_{M\theta}$ and $a_{M\phi}$ show that the acceleration of the missile are still in reasonable scales.

Above all, the simulation results show that actuator faults influence the performance of the guidance law, and the proposed guidance law can get rid of the influence. The results also validate that the designed laws in this study guarantee the missile intercepts the target with impact angle constraint in finite time.

V. CONCLUSIONS

This paper investigates the accurate interception problem and proposes a novel dual-layer adaptive STA-like guidance law in the presence of the impact angle constraint and actuators fault. The presented guidance law is formed by combining STA-like and adaptive theory for the first time to realize accurate interception with impact angle constraint and actuator faults consideration. More specifically, to guarantee the interception, the multi-variable STA-like is adopted in the proposed guidance law drive the line-of-sight (LOS) angle to the desired value and its rate to zero in finite time in both pitch and azimuth directions. To satisfy the demand of the necessary disturbance gradient, owning realistic actuator faults and the independence between missile and target, a multi-variable dual-layer adaptive scheme is employed to adjust the control gains and guarantees its precision. Moreover, the multi-variable dual-layer adaptive scheme can also be adopted to select the proper design parameters.

Comprehensive effectiveness analysis of the proposed guidance law is performed. According to the theoretical investigation, the proposed guidance law can achieve the finite time missile interception with desired impact angles. Furthermore, the developed multi-variable a dual-layer adaptive scheme can get more precisely estimated disturbance information.

Three simulations are implemented in the paper. The first simulation result shows that the proposed guidance law can realize interception with impact angle constraint for different target maneuvers in two directions. The second simulation results shows the presented guidance law can get rid of influence of the different reasonable degrees actuator faults with impact angle constraint in two directions. The last simulation result shows the priority of the proposed guidance law compared with the other two guidance laws. More specifically, the proposed guidance law can lead the missile intercept the target with reasonable accelerations and preferable convergence performances in finite time in the actuator faults consideration. However, the proposed guidance law is carried out on the basis of the theoretical analysis and numerical simulations. Hence, in the future study, we will try to deal with the realistic limits.

APPENDIX

To facilitate the design, some notations are considered for further application.

Notation 1: Throughout this paper, for any given vector $\boldsymbol{x} = [x_1, x_2, \ldots, x_n]^T$, the notations in Table 1 will be used.

More specifically, the sign function is defined as follow,

$$\mathbf{sign}\left(x_j\right) = \begin{cases} 1 & if\ x > 0 \\ 0 & if\ x = 0 \\ -1 & if\ x < 0, \end{cases} \quad (j = 1, 2, \ldots, n) \tag{76}$$

The schur product in the paper is used for a 2×2 matrix with another a 2×2 matrix. For example, the schur product for a 2×2 matrix A with a 2×2 matrix B is:

$$\begin{aligned} A \circ B &= \begin{bmatrix} a_{11} & a_{12} \\ a_{21} & a_{22} \end{bmatrix} \circ \begin{bmatrix} b_{11} & b_{12} \\ b_{21} & b_{22} \end{bmatrix} \\ &= \begin{bmatrix} a_{11}b_{11} & a_{12}b_{12} \\ a_{21}b_{21} & a_{22}b_{22} \end{bmatrix} \end{aligned} \tag{77}$$

TABLE 3. Notation and definition.

Notation	Definition
$\lvert\boldsymbol{x}\rvert=\left[\lvert x_1\rvert,\lvert x_2\rvert,\ldots,\lvert x_n\rvert\right]^T$	absolute value
$\dot{\boldsymbol{x}}=\left[\dot{x}_1,\dot{x}_2,\ldots,\dot{x}_n\right]^T$	time derivative
$\boldsymbol{x}^{-1}=\left[x_1^{-1},x_2^{-1},\ldots,x_n^{-1}\right]^T$	reciprocal value
$\lVert\boldsymbol{x}\rVert=\sqrt{\boldsymbol{x}^T\boldsymbol{x}}$	2-norm
$\mathbf{sign}(\boldsymbol{x})=\left[\mathbf{sign}(x_1),\mathbf{sign}(x_2),\ldots,\mathbf{sign}(x_n)\right]^T$	sign function
$\lambda_{\max}(\boldsymbol{x})=col\left(\lambda_{\max}(x_1),\lambda_{\max}(x_2),\ldots,\lambda_{\max}(x_n)\right)$	maximum values
$\lambda_{\min}(\boldsymbol{x})=col\left(\lambda_{\min}(x_1),\lambda_{\min}(x_2),\ldots,\lambda_{\min}(x_n)\right)$	minimum values
$\circ$	Schur product symbol

Notation 2: For two any given column vector

$$\boldsymbol{A}=[a_1,a_2,\ldots,a_n]^T$$
$$\boldsymbol{B}=[b_1,b_2,\ldots,b_n]^T$$

with same length, $\boldsymbol{A}\geq\boldsymbol{B}$ is defined as that every element in $\boldsymbol{A}$ is larger than or equal to the element in $\boldsymbol{B}$ with the corresponding position, i.e. $a_1\geq b_1, a_2\geq b_2,\ldots,a_n\geq b_n$. For an arbitrary column vectors $\boldsymbol{A}=[a_1,a_2,\ldots,a_n]^T$ and any given constant m, $\boldsymbol{A}\geq m\,(\boldsymbol{A}\leq m)$ means that every element in $\boldsymbol{A}$ is larger (smaller) than or equal to m.

REFERENCES

[1] V. Turetsky and J. Shinar, "Missile guidance laws based on pursuit-evasion game formulations," *Automatica*, vol. 39, no. 4, pp. 607–618, Apr. 2003.

[2] V. Malyavej, I. R. Manchester, and A. V. Savkin, "Precision missile guidance using radar/multiple-video sensor fusion via communication channels with bit-rate constraints," *Automatica*, vol. 42, no. 5, pp. 763–769, May 2006.

[3] N. Harl and S. N. Balakrishnan, "Impact time and angle guidance with sliding mode control," in *Proc. AIAA Guid., Navigat., Control Conf.*, Chicago, IL, USA, Aug. 2009, p. 5897.

[4] K. S. Erer and O. Merttopğuoglu, "Indirect impact-angle-control against stationary targets using biased pure proportional navigation," *J. Guid., Control, Dyn.*, vol. 35, no. 2, pp. 700–704, Mar. 2012.

[5] T.-H. Kim, B.-G. Park, and M.-J. Tahk, "Bias-shaping method for biased proportional navigation with terminal-angle constraint," *J. Guid., Control, Dyn.*, vol. 36, no. 6, pp. 1810–1816, Nov. 2013.

[6] Y. Guo, X. Li, H. Zhang, M. Cai, and F. He, "Data-driven method for impact time control based on proportional navigation guidance," *J. Guid., Control, Dyn.*, vol. 43, no. 5, pp. 955–966, May 2020.

[7] A. Ratnoo and D. Ghose, "Impact angle constrained interception of stationary targets," *J. Guid., Control, Dyn.*, vol. 31, no. 6, pp. 1817–1822, Nov. 2008.

[8] A. Ratnoo and D. Ghose, "Impact angle constrained guidance against nonstationary nonmaneuvering targets," *J. Guid., Control, Dyn.*, vol. 33, no. 1, pp. 269–275, Jan. 2010.

[9] Y.-I. Lee, S.-H. Kim, and M.-J. Tahk, "Optimality of linear time-varying guidance for impact angle control," *IEEE Trans. Aerosp. Electron. Syst.*, vol. 48, no. 4, pp. 2802–2817, Oct. 2012.

[10] X. Chen and J. Wang, "Optimal control based guidance law to control both impact time and impact angle," *Aerosp. Sci. Technol.*, vol. 84, pp. 454–463, Jan. 2019.

[11] L.-J. Liu and Y. Shen, "Three-dimension H_∞ guidance law and capture region analysis," *IEEE Trans. Aerosp. Electron. Syst.*, vol. 48, no. 1, pp. 419–429, Jan. 2012.

[12] W. Wang, S. Xiong, and X. Liu, "Adaptive nonsingular terminal sliding mode guidance law against maneuvering targets with impact angle constraint," *Proc. Inst. Mech. Eng., G, J. Aerosp Eng.*, vol. 229, no. 5, pp. 867–890, Apr. 2015.

[13] S. He and D. Lin, "Continuous robust guidance law for intercepting maneuvering targets," *Trans. Jpn. Soc. Aeronaut. Space Sci.*, vol. 58, no. 3, pp. 163–169, May 2015.

[14] D. Chwa, "Robust nonlinear disturbance observer based adaptive guidance law against uncertainties in missile dynamics and target maneuver," *IEEE Trans. Aerosp. Electron. Syst.*, vol. 54, no. 4, pp. 1739–1749, Aug. 2018.

[15] X. Zhou, W. Wang, Z. Liu, C. Liang, and C. Lai, "Impact angle constrained three-dimensional integrated guidance and control based on fractional integral terminal sliding mode control," *IEEE Access*, vol. 7, pp. 126857–126870, Sep. 2019.

[16] Y. Tian, Y. Cai, Z. Yu, and Y. Deng, "Three-dimensional fast fixed-time convergence guidance law with impact angle constraint," *IEEE Access*, vol. 7, pp. 180467–180481, Dec. 2019.

[17] B. Biswas, A. Maity, and S. R. Kumar, "Finite-time convergent three-dimensional nonlinear intercept angle guidance," *J. Guid., Control, Dyn.*, vol. 43, no. 1, pp. 146–153, Jan. 2020.

[18] S. D. Brierley and R. Longchamp, "Application of sliding-mode control to air-air interception problem," *IEEE Trans. Aerosp. Electron. Syst.*, vol. 26, no. 2, pp. 306–325, Mar. 1990.

[19] B. Kim, J. Lee, H. Han, C. Park, B. Kim, J. Lee, H. Han, and C. Park, "Homing guidance with terminal angular constraint against nonmaneuvering and maneuvering targets," in *Proc. Guid., Navigat., Control Conf.*, New Orleans, LA, USA, Aug. 1997, p. 3474.

[20] T. Yamasaki, S. N. Balakrishnan, H. Takano, and I. Yamaguchi, "Second order sliding mode-based intercept guidance with uncertainty and disturbance compensation," in *Proc. AIAA Guid., Navigat., Control (GNC) Conf.*, Boston, MA, USA, Aug. 2013, p. 5115.

[21] T. Lyul Song and S. Jin Shin, "Time-optimal impact angle control for vertical plane engagements," *IEEE Trans. Aerosp. Electron. Syst.*, vol. 35, no. 2, pp. 738–742, Apr. 1999.

[22] Y. Zhang, M. Sun, and Z. Chen, "Finite-time convergent guidance law with impact angle constraint based on sliding-mode control," *Nonlinear Dyn.*, vol. 70, no. 1, pp. 619–625, Oct. 2012.

[23] S. He and D. Lin, "A robust impact angle constraint guidance law with seeker's field-of-view limit," *Trans. Inst. Meas. Control.*, vol. 37, no. 3, pp. 317–328, Jun. 2014.

[24] S. Kumar, S. Rao, and D. Ghose, "Non-singular terminal sliding mode guidance and control with terminal angle constraints for non-maneuvering targets," in *Proc. 12th IEEE Workshop Variable Struct. Syst.*, Mumbai, India, Jan. 2012, pp. 291–296.

[25] Q. Song and X. Meng, "Design and simulation of guidance law with angular constraint based on non-singular terminal sliding mode," in *Proc. Int. Conf. Solid State Devices Mater. Sci.*, Macao, China, Apr. 2012, pp. 1197–1204.

[26] S. R. Kumar, S. Rao, and D. Ghose, "Nonsingular terminal sliding mode guidance with impact angle constraints," *J. Guid., Control, Dyn.*, vol. 37, no. 4, pp. 1114–1130, Jul. 2014.

[27] J. Zhao and J. Zhou, "Strictly convergent nonsingular terminal sliding mode guidance law with impact angle constraints," *Optik*, vol. 127, no. 22, pp. 10971–10980, Nov. 2016.

[28] P. Lu, D. Doman, and J. Shierman, "Adaptive terminal guidance for hypervelocity impact in specified direction," in *Proc. AIAA Guid., Navigat., Control Conf. Exhibit*, San Francisco, CA, USA, Aug. 2005, p. 6059.

[29] X. Liu and G. Li, "Adaptive sliding mode guidance with impact time and angle constraints," *IEEE Access*, vol. 8, pp. 26926–26932, 2020.

[30] H. Wang, D. Lin, Z. Cheng, and J. Wang, "Optimal guidance of extended trajectory shaping," *Chin. J. Aeronaut.*, vol. 27, no. 5, pp. 1259–1272, Oct. 2014.

[31] F. Yang, C. Wei, N. Cui, and J. Xu, "Adaptive generalized super-twisting algorithm based guidance law design," in *Proc. 14th Int. Workshop Variable Struct. Syst. (VSS)*, Nanjing, China, Jun. 2016, pp. 47–52.

[32] C. Edwards and Y. B. Shtessel, "Adaptive continuous higher order sliding mode control," *Automatica*, vol. 65, pp. 183–190, Mar. 2016.

[33] V. I. Utkin and A. S. Poznyak, "Adaptive sliding mode control with application to super-twist algorithm: Equivalent control method," *Automatica*, vol. 49, no. 1, pp. 39–47, Jan. 2013.

[34] C. Edwards and Y. Shtessel, "Adaptive dual-layer super-twisting control and observation," *Int. J. Control*, vol. 89, no. 9, pp. 1–17, Jun. 2016.

[35] Y. B. Shtessel, I. A. Shkolnikov, and A. Levant, "Guidance and control of missile interceptor using second-order sliding modes," *IEEE Trans. Aerosp. Electron. Syst.*, vol. 45, no. 1, pp. 110–124, Jan. 2009.
[36] Y. Ji, D. Lin, W. Wang, S. Hu, and P. Pei, "Three-dimensional terminal angle constrained robust guidance law with autopilot lag consideration," *Aerosp. Sci. Technol.*, vol. 86, pp. 160–176, Mar. 2019.
[37] Y. Xiaodong and L. Shi, "A novel integral sliding mode-type continuous guidance law with autopilot lag for intercepting non-cooperative maneuvering targets," *IEEE Access*, vol. 7, pp. 126571–126581, 2019.
[38] B. Liu, M. Hou, and D. Feng, "Nonlinear mapping based impact angle control guidance with seeker's field-of-view constraint," *Aerosp. Sci. Technol.*, vol. 86, pp. 724–736, Mar. 2019.
[39] B. Liu, M. Hou, and Y. Li, "Field-of-view and impact angle constrained guidance law for missiles with time-varying velocities," *IEEE Access*, vol. 7, pp. 61717–61727, 2019.
[40] R. H. Chen and J. L. Speyer, "Sensor and actuator fault reconstruction," *J. Guid., Control, Dyn.*, vol. 27, no. 2, pp. 186–196, Mar. 2004.
[41] M. L. Corradini and G. Orlando, "Actuator failure identification and compensation through sliding modes," *IEEE Trans. Control Syst. Technol.*, vol. 15, no. 1, pp. 184–190, Jan. 2007.
[42] M. M. Polycarpou, "Fault accommodation of a class of multivariable nonlinear dynamical systems using a learning approach," *IEEE Trans. Autom. Control*, vol. 46, no. 5, pp. 736–742, May 2001.
[43] S. Yu, X. Yu, B. Shirinzadeh, and Z. Man, "Continuous finite-time control for robotic manipulators with terminal sliding mode," *Automatica*, vol. 41, no. 11, pp. 1957–1964, Nov. 2005.
[44] X.-J. Li and G.-H. Yang, "Robust adaptive fault-tolerant control for uncertain linear systems with actuator failures," *IET Control Theory Appl.*, vol. 6, no. 10, pp. 1544–1551, Jul. 2012.
[45] L. Fei and J. Haibo, "Guidance laws with input constraints and actuator failures," *Asian J. Control*, vol. 18, no. 3, pp. 1165–1172, May 2016.
[46] W. Wang, Y. Ji, D. Lin, Z. Shi, and S. Lin, "A novel approximate finite-time convergent guidance law with actuator fault," *Cluster Comput.*, vol. 9, no. 5, pp. 1–13, Sep. 2017.
[47] S. He, W. Wang, and J. Wang, "Discrete-time super-twisting guidance law with actuator faults consideration," *Asian J. Control*, pp. 1854–1861, Mar. 2017.
[48] S. Li and Y.-P. Tian, "Finite-time stability of cascaded time-varying systems," *Int. J. Control*, vol. 80, no. 4, pp. 646–657, Apr. 2007.
[49] Y. Si and S. Song, "Three-dimensional adaptive finite-time guidance law for intercepting maneuvering targets," *Chin. J. Aeronaut.*, vol. 30, no. 6, pp. 1985–2003, Dec. 2017.
[50] D. Zhou, S. Sun, and K. L. Teo, "Guidance laws with finite time convergence," *J. Guid., Control, Dyn.*, vol. 32, no. 6, pp. 1838–1846, Nov. 2009.

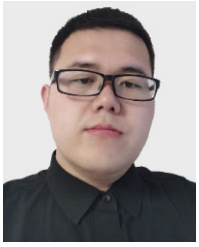

QIANCAI MA was born in Yulin, Shaanxi, China, in 1993. He received the B.S. degree in aerospace engineering from the School of Aerospace Engineering, Beijing Institute of Technology, Beijing, in 2015, where he is currently pursuing the Ph.D. degree. His research interests include flight vehicle guidance and control and advanced control theory.

YI JI was born in Changchun, Jilin, China, in 1994. He received the B.S. and M.S. degrees in aerospace engineering from the School of Aerospace Engineering, Beijing Institute of Technology, Beijing, in 2015 and 2017, respectively, where he is currently pursuing the Ph.D. degree. His research interests include flight vehicle guidance and control and advanced control theory.

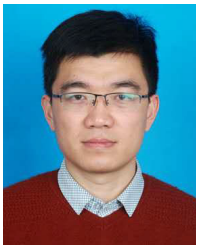

ZHIQI NIU was born in Xuchang, Henan, China, in 1983. He is currently a Senior Engineer with the Xi'an Modern Control Technology Research Institute, Shaanxi, China. He has published seven articles in journals and obtained more than 20 patents. His research interests include flight vehicle design, aerodynamics, and control technology research.

QIUXIONG GOU was born in Liquan, Shaanxi, China, in 1976. He is currently a Senior Engineer with the Xi'an Modern Control Technology Research Institute, Shaanxi, China. He has published eight articles in journals and obtained more than ten patents. His research interests include weapon system application engineering and flight vehicle design.

LIANGYU ZHAO was born in Shangqiu, Henan, China, in 1981. He received the bachelor's and Ph.D. degrees from the Beijing Institute of Technology, Beijing, China, in 2003 and 2008, respectively. He is currently an Associate Professor with the School of Aerospace Engineering, Beijing Institute of Technology. He has published more than 30 papers in journals and conferences. His research interests include flight vehicle design, flight dynamics and control, and aerodynamics.